

Chapter

Study of SPS Sintering of Strontium-Doped Lanthanum Manganite (LSM) by Surface Modification of Powders Using DCSBD and ALD

*Amparo Borrell, Rut Benavente, René M. Guillén,
María D. Salvador, Vaclav Pouchly, Martina Ilcikova,
Richard Krumpolec and Rodrigo Moreno*

Abstract

Throughout the ceramic processing cycle, it is well known that a small change in the surface energy of as-received powders can have a considerable effect on the final properties of consolidated materials. The main objective of this chapter is to describe the design and manufacture of new ceramic materials based on strontium-doped lanthanum manganites, LSM ($\text{La}_{0.8}\text{Sr}_{0.2}\text{MnO}_3$) and LSM-8YTZP composites, for cathode in solid oxide fuel cells (SOFC) applications due to their excellent properties, by modifying the surface energy of the starting powder using techniques, such as Diffuse Coplanar Surface Barrier Discharge (DCSBD) and atomic layer deposition (ALD). Subsequently, in order to evaluate the activation energy and optimise the sintering behaviour of these powders, the Spark Plasma Sintering (SPS) technique will be used. SPS allows the complete densification of pieces by fast and low-energy consumption processing.

Keywords: strontium-doped lanthanum manganites, spark plasma sintering, diffuse coplanar surface barrier discharge, atomic layer deposition

1. Introduction

Strontium-doped lanthanum manganite ($\text{La}_{0.8}\text{Sr}_{0.2}\text{MnO}_3$) materials have a crystal structure of the perovskite-type A-B-O₃, where A and B represent the 12- and 6-coordinated metals, respectively. The $\text{La}_{1-x}\text{Sr}_x\text{MnO}_3$ (LSM) has attracted attention in recent years due to its excellent thermal, electronic and magnetic properties [1] with potential applications in magnetic sensors, readout heads for magnetic memories and as a cathode in solid oxide fuel cells (SOFC) [2].

One of the most important applications of these materials is solid oxide fuel cells. The electrolyte is a ceramic oxide that is generally located in the centre of the cell (although there are exceptions such as in porous metal-supported cells) to facilitate the generation of oxygen vacancies and to transport the ionic charge between the cathode and the anode (**Figure 1**) [3]. The cathode and anode are electrodes where different reactions take place: oxygen is reduced to oxide ions by consuming two electrons at the cathode, and fuel is reduced by forming two electrons at the anode. The electrodes must be porous and facilitate the transport of reactants and products through the different components [4, 5].

The cathode is one of the essential components of a SOFC. The cathode materials must meet several requirements in the operating temperature of 800–1000°C: high electronic conductivity, thermal and chemical stability, catalytic activity for oxygen reduction, and a thermal expansion and coefficients of the same order as the other SOFC components [6, 7].

The use of yttria-stabilised zirconia (Y-TZP) as an electrolyte material is customarily found in the literature, being the main material used for the fabrication of solid electrochemical devices. Its use is due to the fact that this material has high conductivity and ionic stability with oxygen. It is important to emphasise that in solid oxide fuel cells with zirconia as a base material, lanthanum manganites doped with strontium are a key point for better cell efficiency. LSM materials are commonly used as cathode material due to their high electronic conductivity and fast oxygen transfer at gas–solid interfaces, combined with their thermal expansion capability and chemical compatibility with yttria-stabilised zirconia solid electrolyte [8]. The content of yttrium oxide (Y_2O_3) as a dopant for zirconia is a very important factor. In terms of conductivity, zirconia doped with 8–10 mol% yttria has high ionic conductivity. Moreover, in terms of structural and mechanical properties, zirconia doped with 8 mol% yttria has high flexural and impact strength [9]. Therefore, in this chapter, LSM-8YTZP composites will be investigated due to their good mechanical properties [10].

This chapter aims to study how the heating rate, the final temperature and the dwell time affect the final properties of the LSM material and the LSM-8YTZP composite densified using the Spark Plasma Sintering technology. In a second stage, a

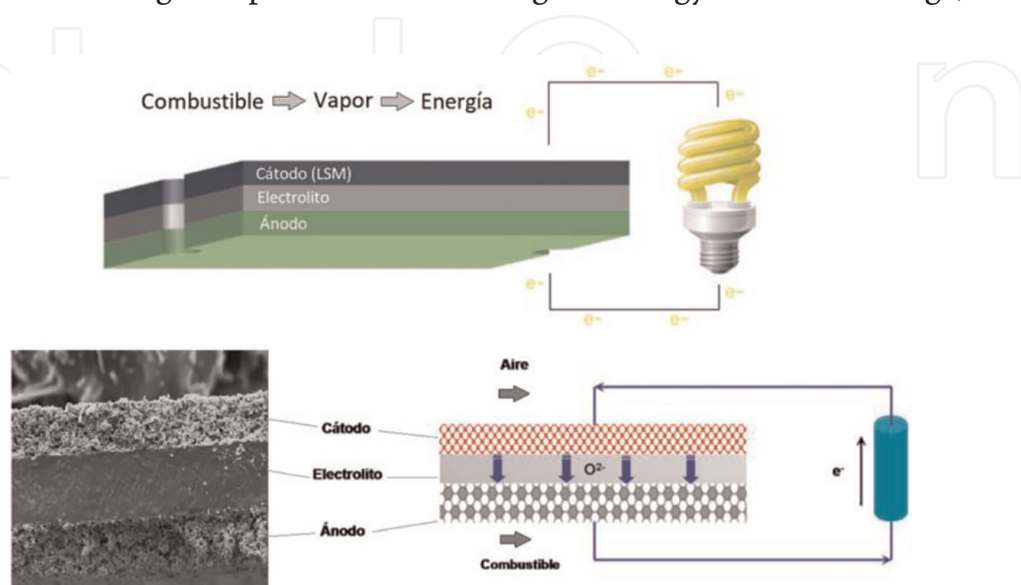


Figure 1.
Diagram of layers forming a SOFC device.

surface modification of the starting powders, both LSM and LSM-8YTZP, will be carried out using Diffuse Coplanar Surface Barrier Discharge (DCSBD) and Atomic Layer Deposition (ALD) techniques in order to identify changes in the material that may influence the sintering and, therefore, the final properties.

2. Materials and methods

2.1 Raw materials

As raw materials, commercial $\text{La}_{1-x}\text{Sr}_x\text{MnO}_3$ ($x = 0.2$) powder (INFRAMAT, Advanced Materials, USA) with an average particle size of $d_{50} = 0.25 \mu\text{m}$, a BET-specific surface area of $2.8 \text{ m}^2/\text{g}$ and high purity commercial yttria-stabilised zirconia (YSZ) with 8 mol% Y_2O_3 (TZ8YS, Tosoh Corp., Japan), with an average particle size of $0.4 \mu\text{m}$, and a BET specific surface area of $4.7 \text{ m}^2/\text{g}$ were used.

The mixture preparation was carried out after optimising the zeta potential of the LSM and 8YTZP suspensions and the rheological behaviour of the LSM-8YTZP mixture. LSM and LSM-8YTZP were prepared as concentrated suspensions in water with a solid loading of 30 vol%. The mixtures were prepared with a volume relative content of 50:50 according to a sequential addition, by first adding the deflocculant required to disperse the 8YTZP (0.5 wt.% on a dry solid basis) and then the 8YTZP powder, followed by the deflocculant required for the LSM (1.5 wt.% on a dry solid basis) before the LSM powder. The optimised slurry of the mixture was then frozen using a rotavapor (IKA, Germany) in a liquid- N_2 bath and subsequently freeze-dried (Cryodos-50, Telstar, Spain) at -50°C and 0.3 mPa vacuum pressure for 24 h to sublimate the ice.

The freeze-dried powders were sintered by Spark Plasma Sintering (SPS, DR. SINTER SPS-625, FUJI, Japan), and the surface energy of this powder was also modified using low-energy techniques such as Diffuse Coplanar Surface Barrier Discharge (DCSBD) and Atomic Layer Deposition (ALD).

Spark Plasma Sintering was carried out under vacuum (5–9 Pa) using a graphite mould with a diameter of 12 mm. The temperature was measured using an optical pyrometer focused on the die wall, a constant uniaxial pressure of 15 MPa was applied above 600°C , and a dwell time of 2 min was used.

2.2 Diffuse coplanar surface barrier discharge (DCSBD)

Diffuse Coplanar Surface Barrier Discharge (DCSBD) is a novel type of atmospheric-pressure plasma source developed for high-speed, large-area surface plasma treatments [11]. The plasma of DCSBD discharge is generated in a sub-millimetre thin layer above the dielectric plate. With a gradual increase of power input, the DCSBD gets visually more and more diffuse and homogeneous, though it is still composed of a high number of individual microdischarges [12–14]. **Figure 2** shows a scheme of the DCSBD electrode system arrangement and a general view of the DCSBD apparatus.

The number of DCSBD microdischarges generated during one discharge period is very high (in the order of tens to hundreds of single microdischarges), and the generated microdischarges are distributed above a large area of approx. $20 \times 8 \text{ cm}^2$. The typical dimensions of a single microdischarge were of the order of 1 mm in length and $100 \mu\text{m}$ in diameter in the time scale of several tens of nanoseconds. The system

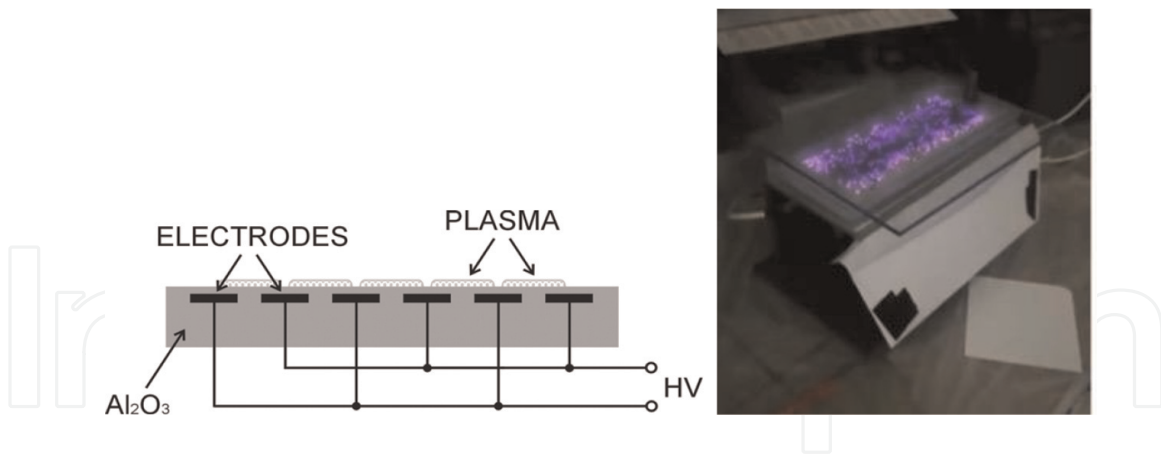


Figure 2. Cross-sectional schematics of DCSBD electrode system arrangement [15] and visual appearance of material with DCSBD apparatus.

was powered by a 14 kHz sinusoidal high voltage of up to 20 kV peak-to-peak amplitude and an input power of 400 W, supplied by a power generator. The powdered material was activated for 45 s and removed for further ceramic processing.

2.3 Atomic layer deposition (ALD)

Atomic layer deposition (ALD) is a method for depositing ultra-thin films with a wide range of applications due to its unique capabilities. This procedure can increase the efficiency of electrical devices by allowing the homogeneous deposition of conformal films with controlled thickness, even on complicated three-dimensional surfaces [16].

The powder was coated in a quartz tube of ID = 20 mm and length 100 mm on both sides, partially sealed by quartz wool. This tube was placed in the centre of a cylindrical deposition chamber diameter of 50 mm and a length of 450 mm. The deposition was done at a chamber pressure of 180 Pa. Pure nitrogen (99.999%) was used as a carrier and purging gas at a total flow rate of 90 sccm (standard cubic centimetres per minute). The zinc oxide coatings were deposited using Diethylzinc (DEtZn, STREM Chemicals) as a metal source and deionised water (Merck Millipore Q-water, 18.2 M Ω) as an oxygen source (**Figure 3**).

Each deposition consisted of 20 ALD cycles starting with H_2O pulse. One ZnO deposition cycle was defined by the following sequence: H_2O pulse (10 s) \rightarrow N_2 purge (30 s) \rightarrow DEtZn pulse (10 s) \rightarrow N_2 purge (30 s). Quite long pulsing and purging times were used due to the deposition of thin coatings on powders. Both DEtZn and H_2O

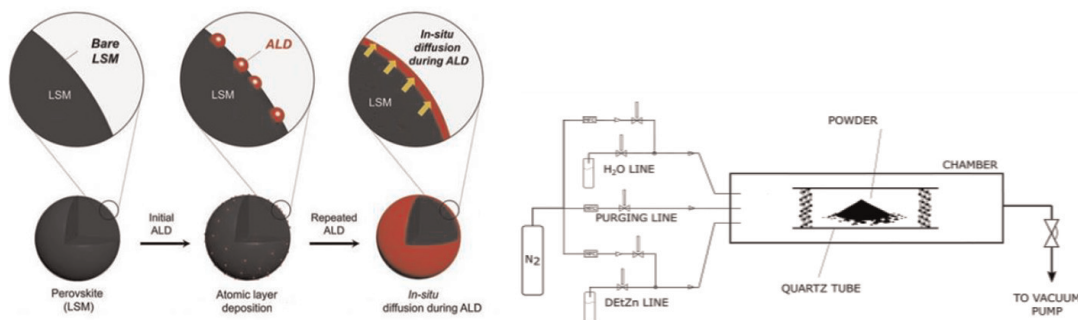


Figure 3. Experimental setup of the ALD coating equipment.

precursors were kept at room temperature. Delivery lines were heated at 60/100°C, and the temperature in the deposition chamber was 140°C. The tube with a coated powder was removed from the deposition chamber always after cooling down to 60°C.

2.4 Characterisation methods

The relative densities of specimens were determined by the Archimedes' method following the ASTM-C-373 standard [17]. Theoretical density values of 6.57 and 6.41 g/cm³ were used for LSM and LSM-8YTZP, respectively, to estimate the relative density of the sintered specimens.

The microstructure and grain size were analysed using field emission scanning electron microscopy (FE-SEM, S4800 Hitachi, Japan). The grain size was measured using the line interception method following the ASTM E112 standard [18], with 10 interception lines being traced in each sample using Image software.

The evaluation of mechanical characteristics (hardness and Young's modulus) was done according to the nanoindentation technique. The method used is a nanoindenter (G-200; Agilent Technologies). Tests were carried out with a Berkovich tip calibrated with silica standard and operated at a maximum depth of 2000 nm. The continuous stiffness measurement was used to determine the contact stiffness and calculate the hardness profiles and elastic modulus [19]. A matrix with 25 indentations was made for every material.

3. Results and discussion

3.1 Study of the LSM powder

3.1.1 LSM sintered by spark plasma sintering

First, a Spark Plasma Sintering (SPS) study of the influence of heating rate on LSM densification was carried out. For this purpose, three heating rates were defined, i.e., 50, 100, and 200°C/min, at a final temperature of 1200°C with a dwell time of 2 min, and a constant uniaxial pressure of 15 MPa was applied above 600°C.

In **Table 1**, the values of average grain size and relative density corresponding to the LSM material sintered by SPS at 1200°C—2 min using different heating rates can be observed.

Small changes are observed with respect to relative density and grain size values. The density value above 90% is reached with a heating rate of 200°C/min. The average grain size is around 1.80 µm, approximately, as can be seen from the microstructure in **Figure 4**. This figure shows the FESEM microstructures, at different

Material	Sintering parameters	Heating rate (°C/min)	Grain size (µm)	Relative density (%)
LSM	1200°C—2 min	50	1.75 ± 0.04	88.0 ± 0.5
		100	1.77 ± 0.05	88.9 ± 0.5
		200	1.85 ± 0.07	90.2 ± 0.5

Table 1.
Grain size and relative density values of LSM material sintered by SPS.

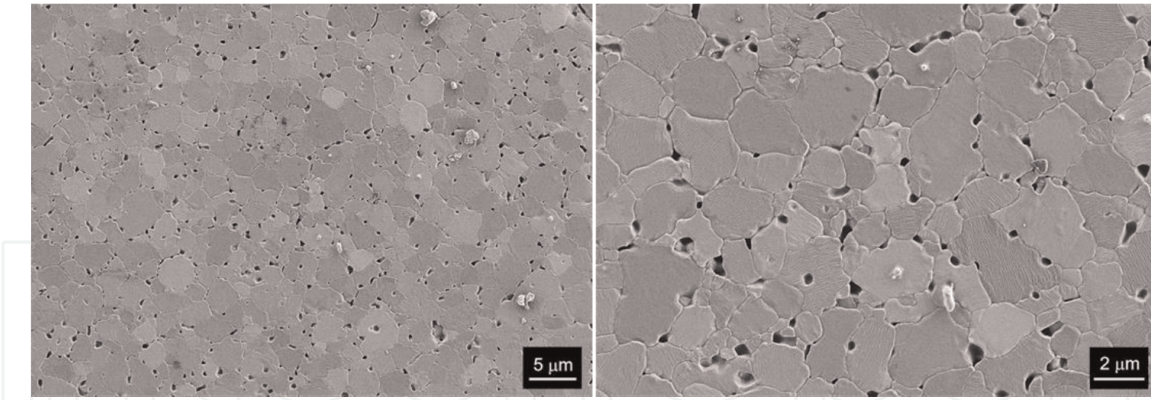


Figure 4.
Microstructure of LSM material sintered by SPS at 1200°C—2 min, heating ramp 200°C/min.

Material	Sintering parameters	Heating rate (°C/min)	Hardness (GPa)	Young modulus (GPa)
LSM	1200°C—2 min	50	7.0 ± 0.3	108 ± 0.2
		100	7.1 ± 0.3	109 ± 0.4
		200	7.5 ± 0.2	120 ± 0.2

Table 2.
Hardness and young modulus values of LSM material sintered by SPS.

magnifications, of polished LSM material sintered by SPS at 1200°C with a heating rate of 200°C/min. It can be observed that large and small grains coexist. In general, all heating rates follow the same tendency, with slightly larger average grain sizes being obtained at higher heating rates, at which higher densification is achieved.

The values of hardness and Young's modulus can be seen in **Table 2**. The Young's modulus values of the material sintered at 50 and 100°C/min show similar values, but a slight increase is observed for the heating rate of 200°C/min. For hardness, an 8% increase is observed when the heating rate is increased from 50 to 200°C/min. This increase is very remarkable, as higher mechanical properties have been achieved at very high heating rates, which influences the total processing cycle of the material. Using a heating rate of 50°C/min, the complete sintering cycle reaches 16 min, and using a heating rate of 200°C/min, it only requires 8 min to complete the sintering cycle. The energy and time savings are therefore doubled.

3.1.2 LSM powders modified by diffuse coplanar surface barrier discharge (DCSBD) and sintered by SPS

The LSM starting powders were modified by the DCSBD technique, using the parameters mentioned in Section 2.2, and then sintered by SPS at 1200°C—2 min, using the same parameters as in the previous section.

In **Table 3**, the values of average grain size and relative density corresponding to the LSM powders modified by DCSBD and sintered by SPS at 1200°C—2 min using different heating rates can be observed.

By means of the DCSBD treatment, it can be identified that the density values of the material change significantly as a function of the heating rate. Density values above 95% are reached, indicating that with this treatment, the density of the final material increases significantly. These density values will have an impact on both the

Material DCSBD	Sintering parameters	Heating rate (°C/min)	Grain size (μm)	Relative density (%)
LSM	1200°C—2 min	50	1.78 ± 0.04	92.7 ± 0.5
		100	1.80 ± 0.03	93.1 ± 0.5
		200	1.75 ± 0.05	95.1 ± 0.5

Table 3.
 Grain size and relative density values of LSM powders modified by DCSBD and sintered by SPS.

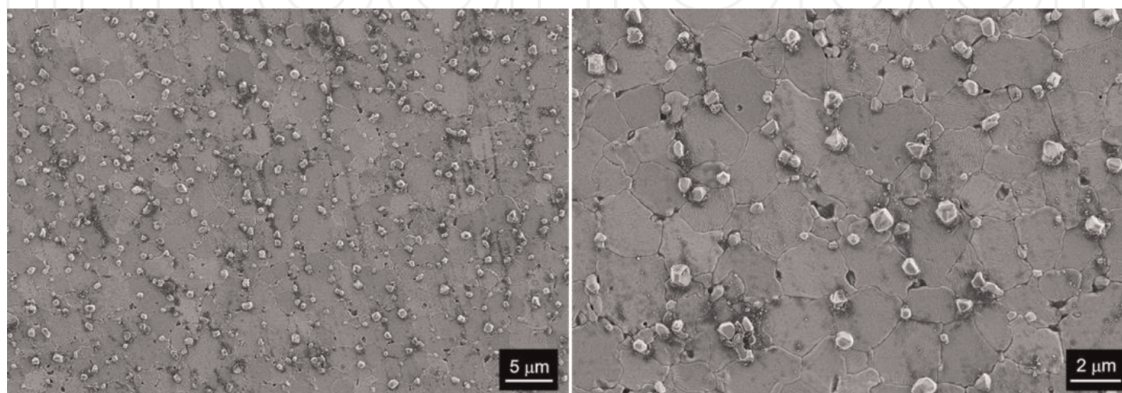


Figure 5.
 Microstructure of LSM material with DCSBD treatment and SPS at 1200°C—2 min, heating ramp 200°C/min.

microstructure and the final mechanical properties. On the other hand, taking into account the grain size values in **Table 1**, it is observed that the materials without any treatment and with DCSBD treatment present similar values. This means that the DCSBD treatment enhances densification while maintaining the same grain sizes.

The FESEM microstructures of the DCSBD-treated sample sintered at 1200°C with a heating rate of 200°C/min, which has a value of 1.75 μm , can be seen in **Figure 5** at different magnifications. Smaller particles of LSM material are observed homogeneously distributed over the entire surface. This may be due to the technique used, as the number of DCSBD microdischarges generated during a discharge period is very high (in the order of tens to hundreds of individual microdischarges), and these generated microdischarges are distributed over a large surface. This surface modification positively influences the densification of the material.

Figure 5 shows a small residual porosity, as the small LSM particles created are located at the grain boundary and help, on the one hand, to close the porosity and, on the other hand, have a tendency to inhibit grain growth.

The values of hardness and Young's modulus can be seen in **Table 4**. The mechanical properties are also influenced by the surface treatment of the powder

Material DCSBD	Sintering parameters	Heating rate (°C/min)	Hardness (GPa)	Young modulus (GPa)
LSM	1200°C—2 min	50	7.7 ± 0.2	124 ± 0.2
		100	7.9 ± 0.2	119 ± 0.4
		200	8.3 ± 0.1	136 ± 0.3

Table 4.
 Hardness and young modulus values of LSM powders modified by DCSBD and sintered by SPS.

before sintering by SPS. Using a heating rate of 200°C/min, hardness values of 8.3 GPa are achieved. Compared to the hardness value achieved with a heating rate of 50°C/min, the improvement is 8%. These hardness values are higher than those shown in **Table 2**, corresponding to the non-treated LSM material. Comparing the LSM material sintered at 1200°C with a heating ramp of 200°C/min, without treatment and the one treated with DCSBD, the difference in hardness values is about 13%. The Young's modulus values achieved using a heating ramp of 200°C/min are around 136 GPa, which represent the highest values obtained. This is in good agreement with the higher densification level.

3.1.3 LSM powders modified by atomic layer deposition (ALD) and sintered by SPS

The LSM starting powders were modified by the ALD technique, using the parameters mentioned in Section 2.3, and then sintered by SPS at 1200°C—2 min, using the same parameters as in the previous section. In **Table 5**, the values of average grain size and relative density corresponding to the LSM powders modified by ALD and sintered by SPS at 1200°C—2 min using different heating rates can be observed.

The final density of the ALD surface-modified LSM sintered using different heating rates is very similar to the non-treated LSM material (**Table 1**). The FESEM microstructures of the ALD-treated sample sintered at 1200°C with a heating rate of 200°C/min, can be seen in **Figure 6**, at different magnifications.

As observed in the microphotographs, a great difference can be seen in the final grain size, which is much higher in these materials treated with the ALD technique. Porosity is observed at the grain boundaries as well as residual porosity in the interior of the grains. The average grain size in all samples is around 2.60 µm. The ZnO layer deposited by this methodology reactivates the surface of the LSM powders, leading to

Material ALD	Sintering parameters	Heating rate (°C/min)	Grain size (µm)	Relative density (%)
LSM	1200°C—2 min	50	2.60 ± 0.03	87.3 ± 0.5
		100	2.57 ± 0.05	88.2 ± 0.5
		200	2.62 ± 0.05	90.5 ± 0.5

Table 5.
Grain size and relative density values of LSM powders modified by ALD and sintered by SPS.

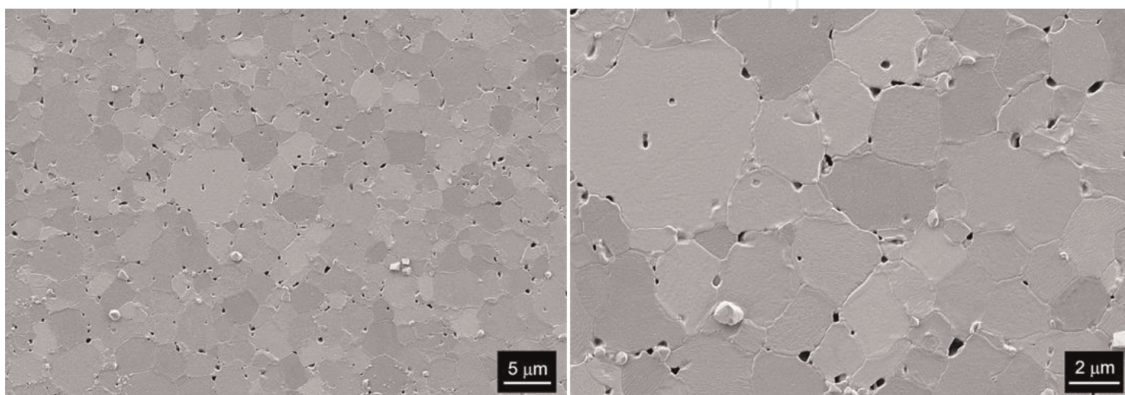


Figure 6.
Microstructure of LSM material with ALD treatment and SPS at 1200°C—2 min, heating ramp 200°C/min.

Material ALD	Sintering parameters	Heating rate (°C/min)	Hardness (GPa)	Young modulus (GPa)
LSM	1200°C—2 min	50	6.1 ± 0.2	92 ± 0.3
		100	5.9 ± 0.3	109 ± 0.3
		200	6.4 ± 0.1	120 ± 0.2

Table 6.
 Hardness and young modulus values of LSM powders modified by ALD and sintered by SPS.

an exaggerated grain growth behaviour in the sintering phase. This grain growth does not help the densification of the material; therefore, the final porosity is around 10%. This will have a negative impact on the mechanical properties, as shown below.

The values of hardness and Young's modulus can be seen in **Table 6**. It is observed, as with the non-treated LSM and the LSM treated with DCSBD, that as the heating ramp values are higher, the mechanical values also show an increase.

The mechanical values indicate that the LSM materials treated with the ALD technique do not lead to an improvement. Comparing the hardness values with those obtained for the non-treated LSM materials (**Table 2**) and those treated with DCSBD (**Table 4**), it can be seen that they are below 7.0 GPa.

If a comparison is carried out between the non-treated LSM materials and those treated with the different DCSBD and ALD techniques, it can be concluded that the treatment that provides the best results is the DCSBD technique. This technique provides lower residual porosity in the material and helps to inhibit grain growth, which leads to superior mechanical properties. In the following section, the influence of surface powder treatment techniques, DCSBD and ALD, on LSM-8YTZP composites will be analysed.

3.2 Study of the LSM-8YTZP powder

3.2.1 LSM-8YTZP sintered by spark plasma sintering

Spark Plasma Sintering (SPS) study of the influence of heating ramps on the LSM-8YTZP material was carried out. For this purpose, the same three heating ramps were defined, i.e., 50, 100, and 200°C/min, at a final temperature of 1200°C with a dwell time of 2 min, applying a constant uniaxial pressure of 15 MPa above 600°C. The obtained results for average grain size and relative density are shown in **Table 7**.

It is observed that as the heating ramp is faster, higher relative density values are achieved. This indicates that rapid heating promotes the densification of these composites. As for the grain size values, all the composites sintered at different heating rates are around 0.36 µm. If these values are compared with those obtained in **Table 1**

Material	Sintering parameters	Heating rate (°C/min)	Grain size (µm)	Relative density (%)
LSM-8YTZP	1200°C—2 min	50	0.30 ± 0.03	92.6 ± 0.5
		100	0.36 ± 0.05	93.1 ± 0.5
		200	0.40 ± 0.02	93.9 ± 0.5

Table 7.
 Grain size and relative density values of LSM-8YTZP composites sintered by SPS.

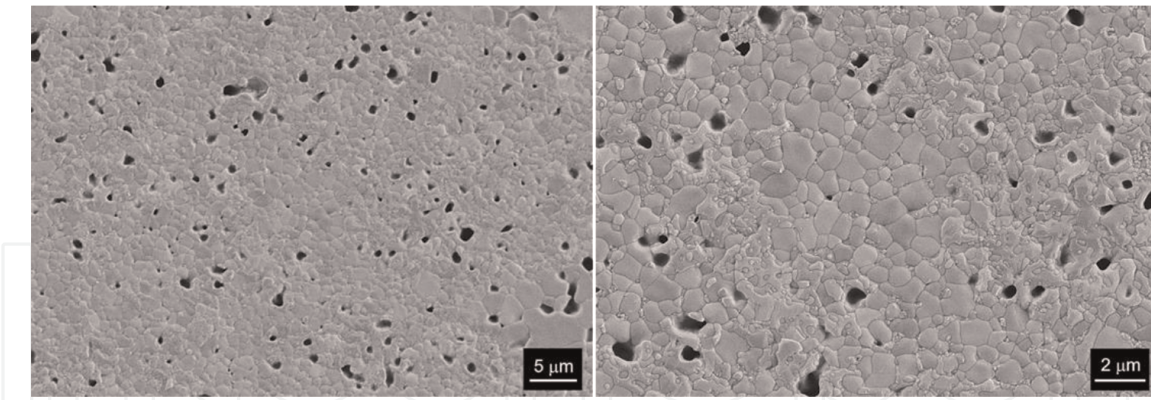


Figure 7. Microstructure of LSM-8YTZP composite sintered by SPS at 1200°C—2 min, heating ramp 200°C/min.

Material	Sintering parameters	Heating rate (°C/min)	Hardness (GPa)	Young modulus (GPa)
LSM-8YTZP	1200°C—2 min	50	10.6 ± 0.2	179 ± 0.2
		100	10.8 ± 0.2	186 ± 0.3
		200	11.2 ± 0.1	190 ± 0.1

Table 8. Hardness and young modulus values of LSM-8YTZP material sintered by SPS.

for the LSM material, they are observed to be 4.5 to be lower, i.e., the 8YTZP zirconia significantly inhibits the grain growth of the LSM.

The FESEM microstructures at different magnitudes of LSM-8YTZP composites sintered at 1200°C with a heating rate of 200°C/min, as shown in **Figure 7**. A homogeneous microstructure is observed. The small zirconia grains are located at the grain boundary inhibiting the growth of LSM grains.

The mechanical hardness and Young's modulus values can be seen in **Table 8**. Hardness values above 11 GPa and Young's modulus values around 190 GPa have been achieved using a heating ramp of 200°C/min. Moratal et al [20] achieved values around 6.0 GPa by sintering this LSM-8YTZP composite by conventional sintering at 1200°C—2 h, heating ramps of 10°C/min. In this study it was found that using the SPS technique almost twice the values of the conventional method were achieved. Another important factor to take into account is that by using SPS, whose heating rate is 200°C/min, the sintering cycle is significantly reduced. Therefore, the high added value of these composites is a very positive factor for their potential industrial applications.

3.2.2 LSM-8YTZP powders modified by diffuse coplanar surface barrier discharge (DCSBD) and sintered by SPS

The LSM-8YTZP starting powders were modified by the DCSBD technique, using the parameters mentioned in Section 2.2, and then sintered by SPS at 1200°C—2 min, using the same parameters as described in Section 3.2.1.

Table 9 shows the values of average grain size and relative density corresponding to the LSM-8YTZP powders modified by DCSBD and sintered by SPS at 1200°C—2 min using different heating rates. As in the case of LSM powders surface-modified by the DCSBD technique, also with LSM-8YTZP powders, the density values increase to more than 95% in the composite sintered at a heating rate of 200°C/min.

Material DCSBD	Sintering parameters	Heating rate (°C/min)	Grain size (μm)	Relative density (%)
LSM-8YTZP	1200°C—2 min	50	0.92 ± 0.03	94.3 ± 0.5
		100	0.94 ± 0.02	94.8 ± 0.5
		200	0.89 ± 0.02	95.8 ± 0.5

Table 9.
 Grain size and relative density values of LSM-8YTZP powders modified by DCSBD and sintered by SPS.

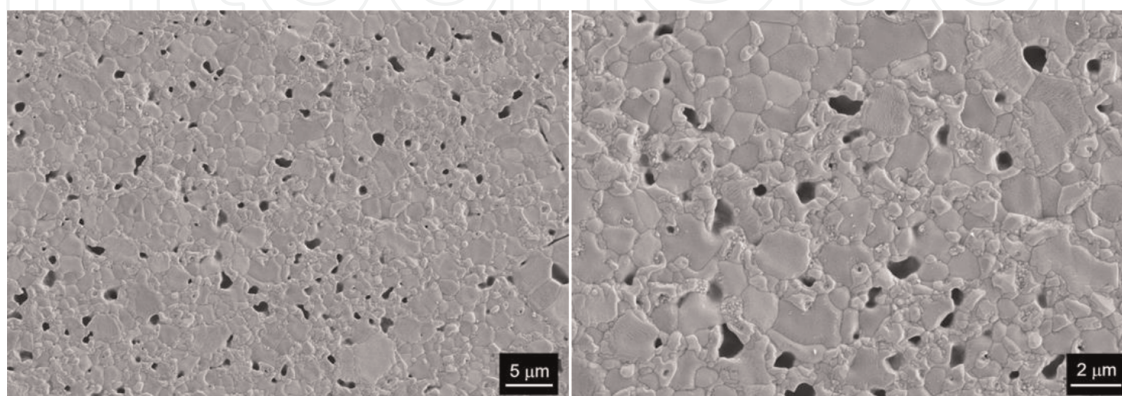


Figure 8.
 Microstructure of LSM-8YTZP composite with DCSBD treatment and SPS at 1200°C—2 min, heating ramp 200°C/min.

The FESEM microstructures at different magnifications of the DCSBD-treated sample sintered at 1200°C with a heating rate of 200°C/min, as shown in **Figure 8**.

The grain size increases slightly in the composites with the modified powders compared to the non-modified ones, and average grain size values of around 0.90 μm are reached. A homogeneous microstructure can be observed, where besides the residual porosity, there is also grain removal due to the polishing process. Small particles of modified powder are situated at the grain boundaries, reinforcing the final material, as seen from the mechanical properties values in **Table 10**.

The LSM-8YTZP composite, sintered at 200°C/min, achieves hardness values of 12.5 GPa. This is very important when compared to the hardness value achieved by the DCSBD-modified LSM material sintered with the same parameters (8.3 GPa). On the one hand, it can be confirmed that the zirconia strengthens the LSM material, and the surface modification by the DCSBD technique also has a very positive effect. The dual effect of the composition and the surface modification increases by 60% both the hardness and the elastic modulus with respect to the untreated LSM material.

Material DCSBD	Sintering parameters	Heating rate (°C/min)	Hardness (GPa)	Young modulus (GPa)
LSM-8YTZP	1200°C—2 min	50	11.0 ± 0.3	188 ± 0.3
		100	11.8 ± 0.2	196 ± 0.1
		200	12.5 ± 0.2	202 ± 0.3

Table 10.
 Hardness and young modulus values of LSM-8YTZP powders modified by DCSBD and sintered by SPS.

3.2.3 LSM-8YTZP powders modified by atomic layer deposition (ALD) and sintered by SPS

The LSM-8YTZP starting powders were modified by the ALD technique, using the parameters mentioned in Section 2.3, and then sintered by SPS at 1200°C—2 min, using the same parameters as in the previous section.

In **Table 11**, the values of average grain size and relative density corresponding to the LSM-8YTZP powders modified by ALD and sintered by SPS at 1200°C—2 min using different heating rates can be observed. These composites reach relative densities very close to those achieved by non-treated composites (**Table 7**), in the order of 93%. The grain size of the composites is similar to that achieved by the materials obtained by DCSBD treatment (**Table 9**).

The FESEM microstructures at different magnifications of the ALD-treated sample sintered at 1200°C with a heating rate of 200°C/min, as shown in **Figure 9**. It can be observed that in the FESEM micrograph obtained at low magnification, there are areas where agglomerates are present, the microstructure is not homogeneous. Residual porosity locates predominantly at the grain boundaries. Zirconia particles have a grain size of 0.3–0.4 μm. These particles inhibit the grain growth of the LSM, and therefore the ALD technique does not have a strong influence on this property. The higher magnification micrograph shows some grain removal due to the polishing phase.

The values of hardness and Young's modulus can be seen in **Table 12**. Hardness values of over 11.0 GPa and an average Young's modulus of around 195 GPa are achieved for all materials. These values are below those achieved when using the DCSBD technique but clearly above those of the LSM treated by ALD. The influence of the microstructure has a key role to play in the final properties.

Material ALD	Sintering parameters	Heating rate (°C/min)	Grain size (μm)	Relative density (%)
LSM-8YTZP	1200°C—2 min	50	0.90 ± 0.04	92.1 ± 0.5
		100	0.92 ± 0.07	92.5 ± 0.5
		200	0.91 ± 0.05	93.4 ± 0.5

Table 11. Grain size and density values of LSM-8YTZP powders modified by ALD and sintered by SPS.

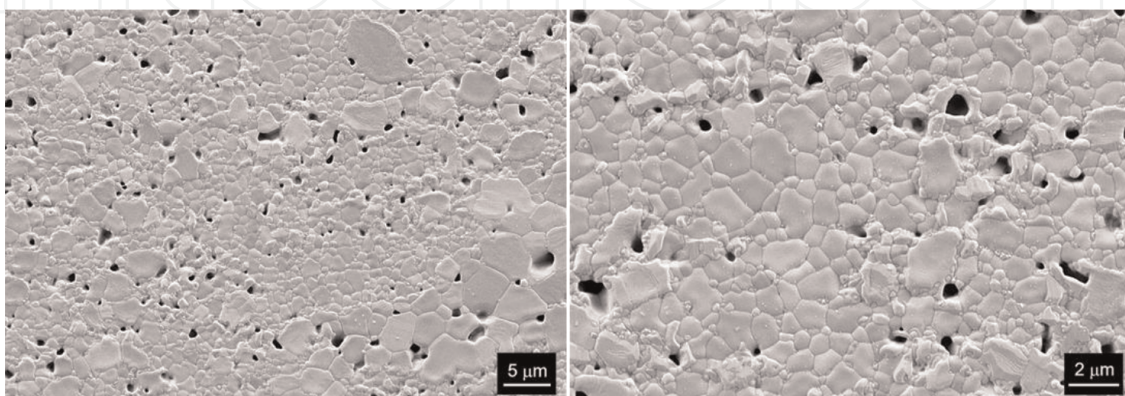


Figure 9. Microstructure of LSM-8YTZP composite with ALD treatment and SPS at 1200°C—2 min, heating ramp 200°C/min.

Material ALD	Sintering parameters	Heating rate (°C/min)	Hardness (GPa)	Young modulus (GPa)
LSM-8YTZP	1200°C—2 min	50	11.2 ± 0.2	190 ± 0.3
		100	11.3 ± 0.2	192 ± 0.4
		200	11.8 ± 0.3	201 ± 0.2

Table 12.
Hardness and young modulus values of LSM-8YTZP powders modified by ALD and sintered by SPS.

4. Conclusions

The addition of zirconia to the LSM material improved its final properties. The LSM material, being very porous, requires higher sintering temperatures to obtain a higher densification. By adding zirconia, the open porosity value of the material is reduced, thus allowing densification at lower working temperatures. In the study carried out, it was identified that with different sintering parameters, the composite material presents different behaviours that can favour some physical properties, depending on the application for which the material is used. In the case of the composite material, when used as a fuel cell, a better interconnectivity between the particles is necessary, so the presence of zirconia is essential. On the other hand, a level of porosity is necessary for the liberation of electrons in the reaction process.

With respect to the LSM and LSM-8YTZP materials, not treated and treated with the different DCSBD and ALD techniques, it can be concluded that the materials that offer the best results are those treated with the DCSBD technique. This technique causes a lower residual porosity in the material and contributes to inhibiting grain growth, which results in superior mechanical properties. The desired improvements are less significant when using the ALD technique.

However, it is important to take into account for future work that the sintering processes in this work were carried out only by SPS, so the modification of the surface may have different results in other non-conventional sintering methods such as microwave, which could be beneficial for the final properties of the materials.

Acknowledgements

Grants PID2021-128548OB-C21 and PID2021-124521OB-100 funded by MCIN/AEI/10.13039/501100011033 and “ERDF A way of making Europe”. Grant CIGE/2021/076 funded by Generalitat Valenciana.

IntechOpen

Author details

Amparo Borrell^{1*}, Rut Benavente¹, René M. Guillén¹, María D. Salvador¹,
Vaclav Pouchly², Martina Ilcikova³, Richard Krumpolec³ and Rodrigo Moreno⁴

1 Instituto de Tecnología de Materiales (ITM), Universitat Politècnica de València,
Valencia, Spain


2 Central European Institute of Technology (CEITEC), Brno, Czech Republic

3 Department of Physical Electronics, Masaryk University, Brno, Czech Republic

4 Instituto de Cerámica y Vidrio, CSIC, Madrid, Spain

*Address all correspondence to: aborrell@upv.es

IntechOpen

© 2023 The Author(s). Licensee IntechOpen. This chapter is distributed under the terms of the Creative Commons Attribution License (<http://creativecommons.org/licenses/by/3.0>), which permits unrestricted use, distribution, and reproduction in any medium, provided the original work is properly cited. 

References

- [1] Zhao S, Wang Y, Zhang Y, Bai J, Zhang Y, Wang S, et al. Enhancement of the redox reactions of the La_{0.8}Sr_{0.2}MnO₃ catalyst by surface acid etching: A simple synthesis strategy to high-performance catalysts for methane combustion. *Fuel*. 2023;**345**: 128258
- [2] Vinchhi P, Khandla M, Chaudhary K, Pati R. Recent advances on electrolyte materials for SOFC: A review. *Inorganic Chemistry Communications*. 2023;**152**: 110724
- [3] Kima HW, Kim HJ, Yun KS, Peck DH, Moon J, Yu JH. Electrochemical characteristics of limiting current sensors with LSM-YSZ and LSM-CGO-YSZ composite electrodes. *Ceramics International*. 2023;**49**:21521-21529
- [4] Li N, Sun L, Li Q, Xia T, Huo L, Zhao H. Novel and high-performance (La,Sr)MnO₃ based composite cathodes for intermediate-temperature solid oxide fuel cells. *Journal of the European Ceramic Society*. 2023;**43**:5279-5287
- [5] Sahini MG, Lupyana SD. Perspective and control of cation interdiffusion and interface reactions in solid oxide fuel cells (SOFCs). *Materials Science & Engineering B*. 2023;**292**:116415
- [6] Borrell A, Salvador MD. Advanced ceramic materials sintered by microwave technology. *Sintering Technology - Method and Application*. Ed. Intech Open. 2018;**1**:3-24. DOI: 10.5772/intechopen.78831
- [7] Manishanma S, Dutta A. Synthesis and characterization of nickel doped LSM as possible cathode materials for LT-SOFC application. *Materials Chemistry and Physics*. 2023;**297**:127438
- [8] Budác D, Milos V, Carda M, Paidar M, Fuhrmann J, Bouzek K. Prediction of electrical conductivity of porous composites using a simplified Monte Carlo 3D equivalent electronic circuit network model: LSM-YSZ case study. *Electrochimica Acta*. 2023;**457**: 142512
- [9] Gupta N, Mallik P, Lewis MH, Basu B. Improvement of toughness of Y-ZrO₂: Role of dopant. *Distribution*. 2004;**268**: 817-820
- [10] Moratal S, Guillén R, Salvador MD, Benavente R, Peñaranda-Foix FL, Moreno R, Borrell A. Comparative study of mechanical and microstructural properties of LSM ceramics obtained by E-field and H-field, AMPERE 2021 - 18th International Conference on Microwave and High Frequency Heating, Conference Paper, Code 176575
- [11] Čech J, Hanusová J, Šťáhel P, Černák M. Diffuse coplanar surface barrier discharge in artificial air: Statistical behaviour of microdischarges. *Open Chemistry*. 2015;**13**:528-540
- [12] Skácelová D, Danilov V, Schäfer J, Quade A, Šťáhel P, Černák M, et al. Room temperature plasma oxidation in DCSBD: A new method for preparation of silicon dioxide films at atmospheric pressure. *Materials Science and Engineering B*. 2013;**178**: 651-655
- [13] Prysiashnyi V, Vasina P, Panyala NR, Havel J, Cernak M. Air DCSBD plasma treatment of Al surface at atmospheric pressure. *Surface and Coatings Technology*. 2012;**206**: 3011-3016
- [14] Pouchlý V et al. Improved microstructure of alumina ceramics

prepared from DBD plasma activated powders. *Journal of the European Ceramic Society*. 2019;**39**:1297-1303

[15] Černák M, Černáková L, Hudec I, Kováčik D, Zahoranová A. Diffuse Coplanar Surface Barrier Discharge and its applications for in-line processing of low-added-value materials. *European Physical Journal: Applied Physics*. 2009; **47**(2):1-6. DOI: 10.1051/epjap/2009131. hal-00497324

[16] Justin Kunene T, Kwanda Tartibu L, Ukoba K, Jen T-C. Review of atomic layer deposition process, application and modeling tools. *Materials Today Proceedings*. 2022;**62**:S95-S109

[17] ASTM C373–14. Standard Test Method for Water Absorption, Bulk Density, Apparent Porosity, and Apparent Specific Gravity of Fired Whiteware Products, ASTM C373–88. 88 (1999) 1–2

[18] ASTM E112. Standard Test Methods for Determining Average Grain Size E112–10, ASTM E112–10. 96 (2010) 1–27

[19] Oliver WC, Pharr GM. An improved technique for determining hardness and elastic modulus using load and displacement sensing indentation experiments. *Journal of Materials Research*. 1992;**19**:1564-1583

[20] Moratal S, Benavente R, Salvador MD, Peñaranda-Foix FL, Moreno R, Borrell A. Microwave sintering study of strontium-doped lanthanum manganite in a single-mode microwave with electric and magnetic field at 2.45 GHz. *Journal of the European Ceramic Society*. 2022;**42**: 5624-5630